Thermo-Responsive Iron Oxide Nanocubes for an Effective Clinical Translation of Magnetic Hyperthermia and Heat-Mediated Chemotherapy

Binh T. Mai* [a,b], Preethi Bala Balakrishnan* [a,b], Markus J. Barthel[a], Federica Piccardi[a], Dina Niculaes[a,b], Federica Marinaro[a,c], Soraia Fernandes[a], Alberto Curcio[a], Hamilton Kakwere[a], Gwennhael Autret[e], Roberto Cingolani[a], Florence Gazeau[d], and Teresa Pellegrino[a]**

[a]Istituto Italiano di Tecnologia, via Morego 30, 16145, Genoa, Italy

[b]Dipartimento di Chimica e Chimica Industriale, Università di Genova, Via Dodecaneso, 31, 16146 Genova, Italy

[c]Currently: The Gurdon Institute and Dept. of Biochemistry, University of Cambridge, Tennis court road, Cambridge CB2 1QN, UK

[d]Laboratoire Matière et Systèmes Complexes, UMR 7057, CNRS and University Paris Diderot, 75205 Paris Cedex 13, France

[e]Centre de Recherche Cardiovasculaire de Paris 56, rue Leblanc75737 PARIS Cedex 15, France

* these authors have contributed equally to this work

** corresponding author: Teresa.pellegrino@iit.it

1. Experimental sections

1.1. Synthesis of the initiator 2-Bromo-N-[2-(3,4-dihydroxy-phenyl)-ethyl] propionamide (DOPA-BiBA)

The catechol-functionalized initiator (DOPA-BiBA) was synthesized following a procedure that was reported elsewhere, with minor modifications.[1] Namely, borax ($Na_2B_4O_7 \cdot 10\ H_2O$, 11.5 g, 30.0 mmol) was dissolved in 300 mL water in a 500 mL round-bottom flask. The solution was degassed using a nitrogen flow for 30 min and DOPA.HCl (5.7 g, 30.0 mmol) was added under nitrogen. The reaction mixture was stirred for 15 min and Na_2CO_3 (12.0 g, 113.2 mmol) was added to adjust the pH to 9-10. Then the solution was cooled using an ice bath and 2-bromoisobutyryl bromide (2- BiBA, 3.7 mL) was injected dropwise using a syringe. The reaction was allowed to proceed overnight under a nitrogen flow. The mixture was acidified to reach pH 2 with a concentrated HCl solution and extracted with ethyl acetate (3×150 mL). The extracted phase was dried over $MgSO_4$ and the solvent was removed by vacuum distillation to yield a brownish viscous liquid, which was further purified by column chromatography (SiO_2, 4 % methanol in chloroform). The obtained yellowish viscous liquid was recrystallized at -20 °C for 48 h. The crystallites were washed several times with dichloromethane and dried in a vacuum oven to collect the pure product as white crystals (purity > 95%). ^{1}H NMR (400 MHz, DMSO-d_6) ppm: 8.72 (s, 1H) and 8.62 (s, 1H) - hydroxyl (OH) of catechol; 8.05 (t, 1H, -H_2C-N**H**-C(O)-); 6.63 (d, 1H), 6.58 (d, 1H) and 6.44 (d, 1H) - aromatic ring; 3,22 (m, 2H, -C**H**$_2$-CH_2-NH-); 2.55 (t, 2H, -CH_2-C**H**$_2$-NH-); 1.85 (s, 6H, Br-C(C**H**$_3$)-C(O)-NH-).

1.2. Determination of the DOXO-loading efficiency of TR-cubes by DMSO release and calibration of DOXO in saline

DMSO release was employed to calculate the loading content of DOXO. In detail, 10 µL of DOXO loaded TR-cubes in saline (2.5 g.L^{-1}) was diluted with 90 µL of DMSO in a 250 µL Eppendorf Falcone tube. The supernatant was collected by magnetic decantation and subjected to UV-vis measurements. The spectrum of the supernatant was shown in Figure S5c. The absorption peak at 501 nm was used to calculate the absolute amount of DOXO using a calibration curve of DOXO in a DMSO:Saline (90:10) mixture. The DOXO concentrations used for the calibration curve were 7, 14, 28, 56, 112 and 225 µg.mL^{-1}. The absorption peak value at 501 nm was plotted against the concentrations. Based on that, a loading efficiency of 9.4% was determined.

A calibration curve of DOXO in saline was also prepared for the DOXO release experiment. The concentrations of DOXO in saline used for calibration were 4, 8, 16, 32, 64 and 128 $\mu g.mL^{-1}$. The absorption peak at 480 nm was used for calibration (Figure 5c).

1.3. DOXO release at room temperature

100 µL of solution containing DOXO-loaded TR-cubes (47 µg DOXO per each mg iron, iron concentration 2.5 $g.L^{-1}$) in a 250 µL Eppendorf tube was kept at room temperature for 24h and placed at the corner of a cubic shaped rare-earth magnet. In the first release, 50 µL of the supernatant was taken after 48 h. Then 50 µL of fresh saline was added and the solution was sonicated for 10 s so that the TR-cubes would be re-dispersed. The mixture was then kept for 24 h on top of a magnet (0.3T). This process was repeated 5 times and all the collected supernatants were quickly subjected to UV-vis absorption measurements in order to evaluate the amount of DOXO in solution.

1.4. DOXO release experiments under an alternating magnetic field-hyperthermia (AMF)

100 µL of the same solution of DOXO-loaded-TR-cubes (47 µg DOXO per each mg iron, iron total concentration 2.5 $g.L^{-1}$) was used for the drug release under an AMF. In detail, 100 µL of the sample was placed in a 250 µL Eppendorf tube, then exposed to an alternating magnetic field for 30 min (11 kAm^{-1} and 105 kHz). Supernatants were collected and fresh media was refilled using the aforementioned methods for the experiment performed at room temperature. The DOXO release under an AMF was repeated 8 times and the DOXO amount was calculated based on UV-vis absorption spectra.

1.5. Effect of heat on chemotherapeutic efficiency of DOXO

To test the ability of DOXO to maintain its chemotherapeutic effect after heat exposure, we subjected DOXO to various temperature (37ºC, 42 ºC and 50 ºC) at different exposure time (30min and 90min). Different concentration of DOXO in water, 4, 2, 1, 0.75 and 0.5µg/mL were taken in tinted glass vials and placed in water bath set to conditions 37ºC (untreated DOXO), 42ºC for 30min, 42ºC for 90min (similar heat as our in vivo MH conditions) and also 50ºC for 30min. After respective heating cycles, the heated DOXO solution was added to cell media kept at 37ºC and incubated with A431 epidermoid carcinoma cells for 24h and 48h time periods. After these incubation periods, the media containing the DOXO were removed and the wells were washed thoroughly with PBS to remove any unbound DOXO, after which they were replaced by fresh media containing

10% PrestoBlue® working solution (Invitrogen™) and incubated at 37ºC for 2 h. Then 100µL of supernatant was transferred to a new 96 well plate and absorbance was read at 570nm and 600nm (background) using MultiSkan™ GO Microplate Spectrometer (Thermofisher™). The % viability was then calculated, normalizing each condition to control untreated cells, and the mean value was plotted with the Standard Deviation (SD). All experiments were done in triplicate (n=3).

1.6. *In vitro* biocompatibility assay

To access the biocompatibility of the nanocubes, A431 cells, plated in a 24 well plate, were incubated with two different concentrations of pristine TR-cubes alone (0.25 and 0.50 gL^{-1} Fe in 500µL media) for 24 and 48 h. After these incubation periods, the media containing the nanocubes were removed and the wells were washed thoroughly with PBS to remove any unbound iron, after which they were replaced by fresh media containing 10% PrestoBlue® working solution (Invitrogen™) and incubated at 37ºC for 2 h. Then 100µL of supernatant was transferred to a new 96 well plate and absorbance was read at 570nm and 600nm (background) using MultiSkan™ GO Microplate Spectrometer (Thermofisher™). The % viability was then calculated, normalizing each condition to control untreated cells, and the mean value was plotted with the Standard Deviation (SD). All experiments were done in triplicate (n=3).

1.7. Humane sacrifice and storage of collected organs

The animals were sacrificed when one of their tumor dimensions reached approx. 2cm (accepted humane endpoint). The animals were anesthetized using an isoflurane gas system and euthanized by a slow influx of CO_2. After sacrificing the animals, the tumor, liver, kidneys and spleen were resected surgically without damaging the organs. These were then fixed in 4% sterile paraformaldehyde for 3-4days and transferred to 20% sucrose. The organs were then stored in sucrose for further use at 4ºC.

1.8. Tissue embedding and Tissue cutting

The organs stored in sucrose were drained and blotted to remove the sucrose, and subsequently embedded in O.C.T (Tissue-Tek® O.C.T. Compound, Sakura® Finetek). Frozen OCT embedded tissues were mounted in the cryostat (Cryotome™) sample holder and slices were cut to 10µm thickness and collected in glass slides (Superfrost Ultra Plus® from Themofisher Scientific™). The tissue slices that were contained in glass slides were stored at -20ºC.

1.9. Histopathological analysis

Tissue slices were rehydrated in PBS. Meanwhile, a Prussian Blue staining reagent for iron was prepared by mixing equal volumes of 20% aqueous solution of hydrochloric acid (Sigma-Aldrich) and 10% aqueous solution of potassium hexacyanoferrate (III) (Sigma-Aldrich). The slides were then dipped in the Prussian blue staining solution for 20min, followed by thorough washing in distilled water. The nucleus of the cells comprising the tissue was counterstained using Fast red (Sigma-Aldrich®) for 5min, then rinsed 2 times in distilled water. Dehydration of the tissues was performed by first immerging them in 95% alcohol then in 100% alcohol. A coverslip was applied to the slides using a resinous mounting medium (Eukitt® Quick hardening mounting medium). Then, the slices were examined using a light microscope (Eclipse Ni-U upright microscope, Nikon®) at 10X and 20X magnification, which also facilitated a full virtual tissue reconstruction.

2. Characterization techniques

2.1. Nuclear Magnetic Resonace (NMR)

NMR spectra were measured using Bruker Ultra Shield Avance spectrometers 400 MHz. For NMR analyses, deuterated chloroform ($CDCl_3$) was used as the solvent to measure the polymers while DMSO-d_6 was used to measure DOPA-BiBA.

2.2. Size Exclusion Chromatography (SEC)

SEC was performed in order to study the molar mass of the polymers. The measurements were carried out on an Agilent 1260 Infinity quaternary LC system consisting of an Agilent 1260 Infinity quaternary pump (G1311B), autosampler (G1329B), two PLGel 5μm MIXED-C columns (kept at 25 °C) and a refractive index detector (G1362A). THF was used as the eluent at a flow rate of 1 mL/min. The SEC system was calibrated using Agilent narrow molar mass distribution polystyrene standards in THF.

2.3. Dynamic Light Scattering (DLS)

Particle sizes were characterized by dynamic light scattering (DLS) using a Malvern Instruments Zetasizer nano series instrument. An equilibration time of 2 min was allowed prior to each measurements and at least three replicate measurements were made for each sample ([Fe] = 25 ppm).

2.4. Transmission Electron Microscopy (TEM)

TEM images were recorded using a JEOL JEM 1011 electron microscope, which worked at an acceleration voltage of 100 kV and was equipped with a W thermionic electron source and a 11Mp Orius CCD Camera (Gatan company, USA). Samples were prepared by placing a drop of the sample onto a carbon coated copper grid which was then left to dry before imaging.

2.5. Fourier Transform Infrared (FT-IR)

FT-IR spectra were recorded using a Bruker vertex 70v Fourier transform infrared spectrometer. Samples were prepared by placing a drop of the sample onto a silicon wafer and leaving it to dry in a desiccator at room temperature overnight before analysis.

2.6. Turbidimetric Analysis

Turbidimetric analyses were done using a Varian Cary 5000 UV−vis spectrophotometer equipped with Peltier elements for temperature control. Measurements were done on solutions of ~ 25 ppm (Fe), and the sample was left to equilibrate at the desired temperature for 3 min before each recording. The transmittance was recorded at 650 nm to avoid the interference of iron oxide nanoparticles.

2.7. Elemental Analysis

Elemental analysis was carried out *via* Inductively Coupled Plasma (ICP) Atomic Emission Spectroscopy on a ThermoFisher CAP 6000 series. The samples were prepared by digesting 10 µL of sample in 1.0 mL of aqua regia overnight then diluting it with 10 mL Milli-Q water.

2.8. UltraViolet-visible (UV-vis) absorption spectroscopy

UV-vis absorption spectra were recorded by a Varian CARY 300 Scan UV–visible spectrophotometer. The UV-vis absorbance measurements were carried out in the wavelength range of 350–700 nm.

2.9. Hyperthermia Measurements

All the measurements were carried out by a commercially available DM100 Series (NanoScale Biomagnetics Corp.) setup. For instance, 100 µL of the sample was introduced to a sample holder and exposed to an AC magnetic field at a frequency (105 kHz) and magnetic field amplitudes 11 $kA.m^{-1}$. All reported SAR values and error bars

were calculated from the mean and standard deviation, respectively, of at least four experimental measurements. SAR values were calculated according to the equation

$$\mathrm{SAR}\left(\mathrm{W.g}^{-1}\right) = \frac{\mathrm{C}}{\mathrm{m}} \times \frac{\mathrm{dT}}{\mathrm{dt}}$$

in which C is the specific heat capacity of the solvent (C_{water} = 4185 $JL^{-1}.K^{-1}$) and m is the concentration ($g.L^{-1}$ of Fe) of magnetic material in solution. Note that the final values are reported as ($W.g^{-1}Fe$). The measurements were carried out under non-adiabatic conditions; thus, the slope of the curve $dT.dt^{-1}$ was measured by taking into account only the first few seconds of the curve.

Supplementary Figures

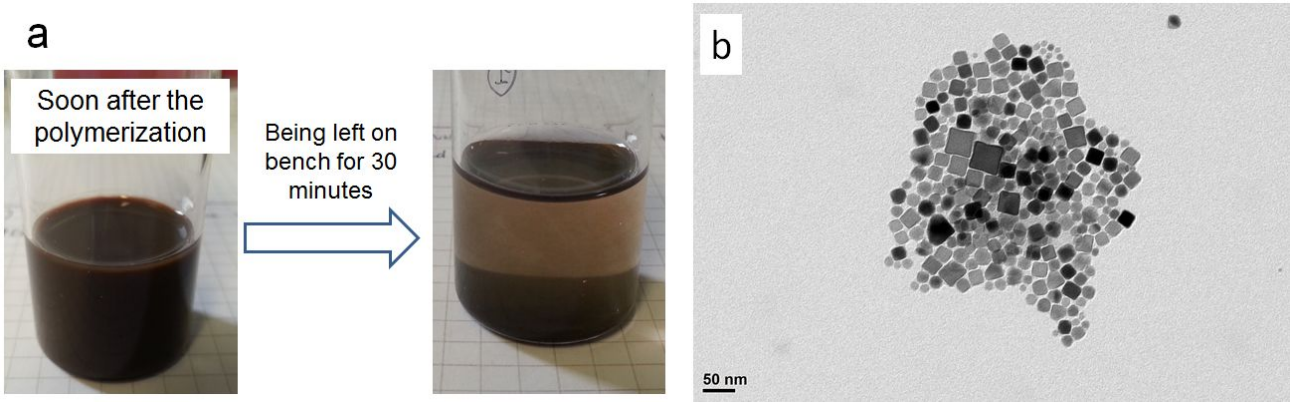

Figure S1. Trial for the synthesis of TR-cubes using classical ATRP. a. The digital photos show that the TR-cubes have a strong tendency to sediment after polymerization. **b.** A representative TEM image revealing the severely aggregated state of the TR-cubes upon workup and being dissolved in water.

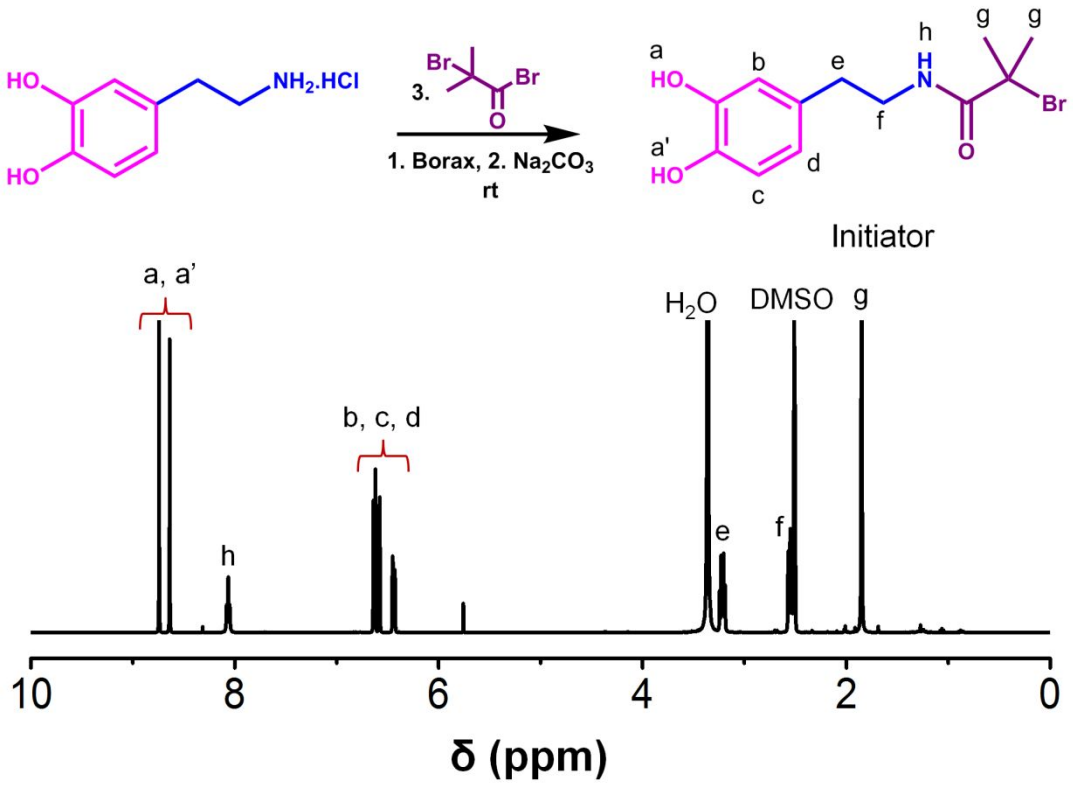

Figure S2. Synthesis and characterization of initiator. Synthetic scheme and ^{1}H NMR spectrum (DMSO-d_6) of initiator. δ (ppm): 8.74 (1H, singlet, a); 8.64 (1H, singlet, a'); 8.06 (1H, triplet, h); 6.63 (1H, doublet, d); 6.58 (1H, doublet, b); 6.44 (1H, quadruplet, c); 3.22 (2H, quadruplet, e); 2.55 (2H, triplet, f); 1.85 (6H, singlet, g).

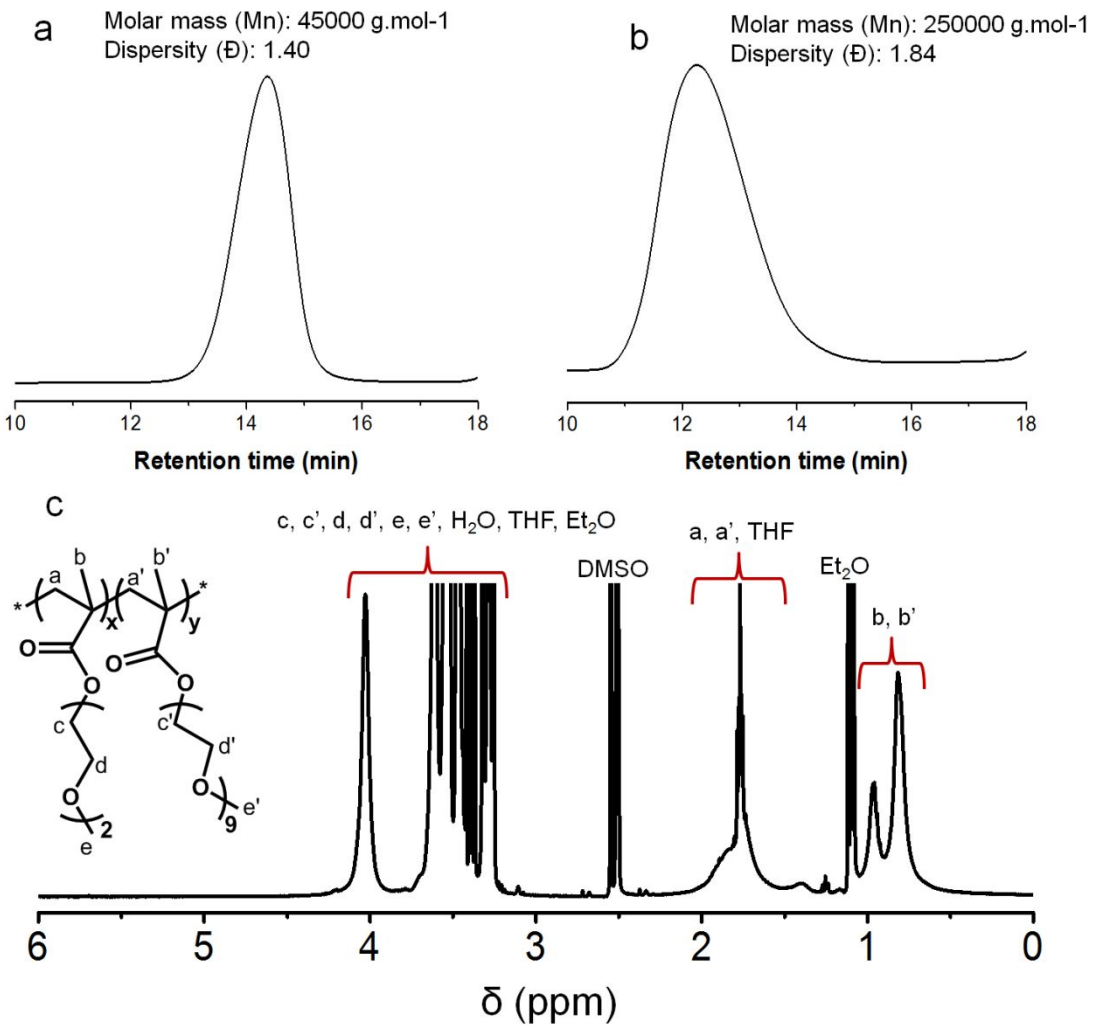

Figure S3. Polymer characterization by NMR and SEC. At the end of the PI-CMRP reaction, after the magnetic collection of the TR-cubes (21 nm nanocubes), the unbounded polymer chains present in the reaction pot were used as a representative sample for the polymer characterization. **a-b.** Size exclusion chromatography (SEC) traces of unbounded polymers suggests a molar mass of 45000 g/mol and a dispersity index of 1.4 for 2.5 h of polymerization. **a.** A molar mass of 250000 g/mol and a dispersity index of 1.84 for 5 h of polymerization. **b.** Eluent: THF, Standard: Polystyrene. **c.** ^{1}H NMR spectrum of unbounded polymers (DMSO). The signals from 4.20 to 3.20 ppm are assigned to the magnetic resonance of the proton in ethylene glycol-based side chains (-O-C**H**$_2$-C**H**$_2$-O-, -O-C**H**$_3$). In this region, there are also THF signals, ethyl ether (Et_2O) coming from the workup step and H_2O from deuterated DMSO. The signals from 1.05 to 0.60 ppm are assigned to the methylene protons (-C**H**$_2$-) in the polymer backbones while the signals from 2.30 and 1.30 are assigned to the methyl proton (-C**H**$_3$) in the polymer backbones.

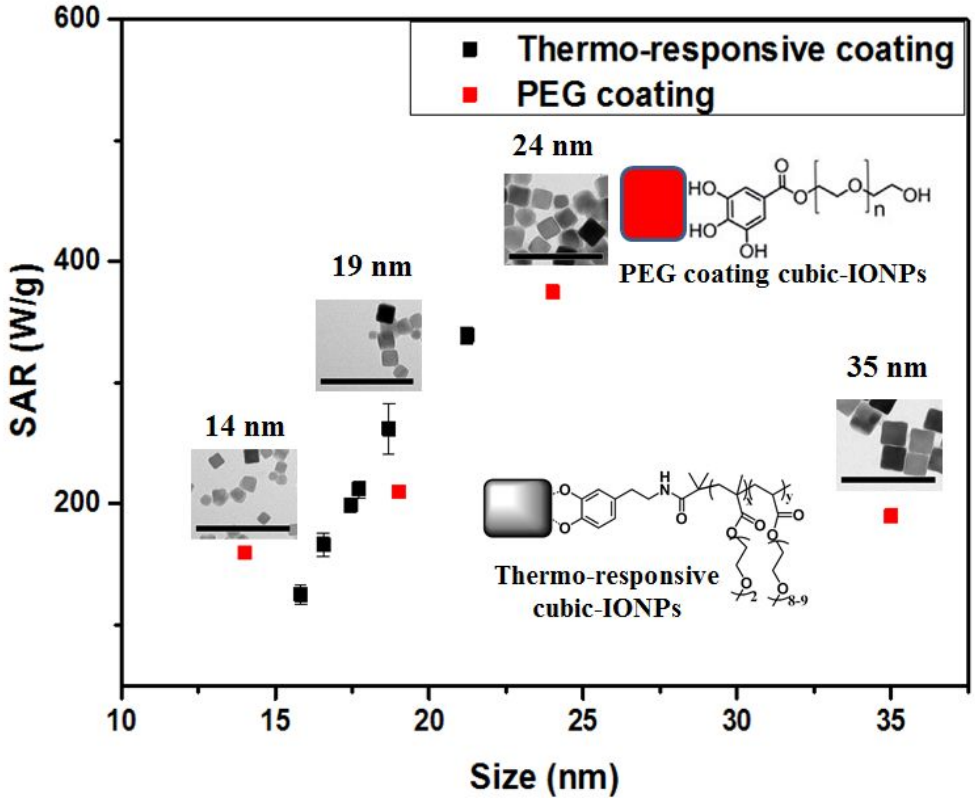

Figure S4. Comparison between TR-cubes and IONCs with a standard PEG coating. SAR values as a function of cube edge for TR-cubes coated with thermo-responsive polymer (black square, Mn: 45000 g.mol-1) and coated with standard PEG bearing catechol (PEG-cubes, red square, Mn = 3000 g.mol-1) polymers. The result shows that the SAR values of TR-cubes and PEG-cubes are comparable. In some cases a maximum difference of 15% in SAR value can be observed. The higher SAR of TR-cubes than PEG-cubes might be due to a better stability of the TR-cubes since they have a better polymer packing having the polymer grown in situ from the surface. In the case of the PEG-cubes a ligand exchange process is used, and the pre-formed polymer might be less efficient in packing at the nanoparticle surface thus slightly affecting the stability and in turn, the SAR values.

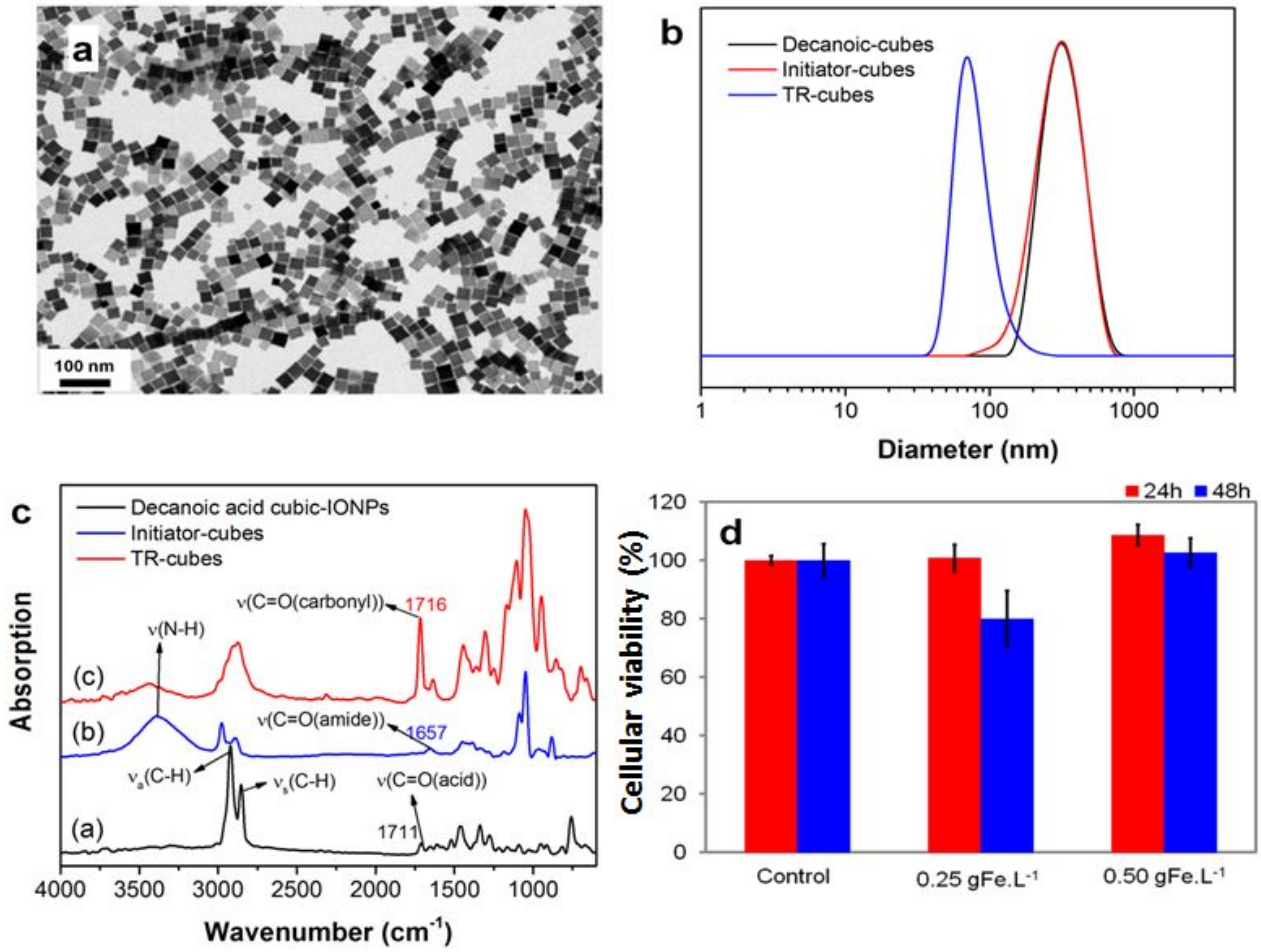

Figure S5. **Colloidal stability, surface composition and biocompatibility characterization of the TR-cubes**. **a.** Representative TEM image of pristine cubes coated with decanoic acid showing an aggregating tend. **b.** Comparison of hydrodynamic diameters (number-weighted) measured by DLS on decanoic acid capped cubes (black line, in $CHCl_3$), initiator-modified cubes (blue line, in THF) and TR-cubes (red line, in PBS). **c.** FT-IR spectra of decanoic acid capped cubes (black), initiator-modified cubes (blue) and final TR-cubes (red). The characteristic absorption bands of the alkyl stretching (-C-H) at 2852-2952 cm^{-1} and carbonyl stretching (>C=O) at 1711 cm^{-1} were clearly visible for the initial cubes coated with decanoic acid (black curve). Upon ligand exchange the appearance of a peak at 1657 cm^{-1} that could be attributed to the amide carbonyl stretching (-N>C=O) indicate the replacement of the initial decanoic acid with initiator (blue curve). FT-IR spectrum of the thermo-responsive cubic-IONPs showed the existence of two strong peaks at 1716 cm-1 and 1051 cm-1, which are ascribable to the ester carbonyl (-O-C=O) and ether (-C-O-C) groups of the bounded polymer indicating a successful functionalization. **d**. viability on A431 cells by a PrestoPrestoBlue® assay for TR-cubes after 24 h and 48 h of incubation at 0.25 and 0.5 $g_{Fe}L^{-1}$.

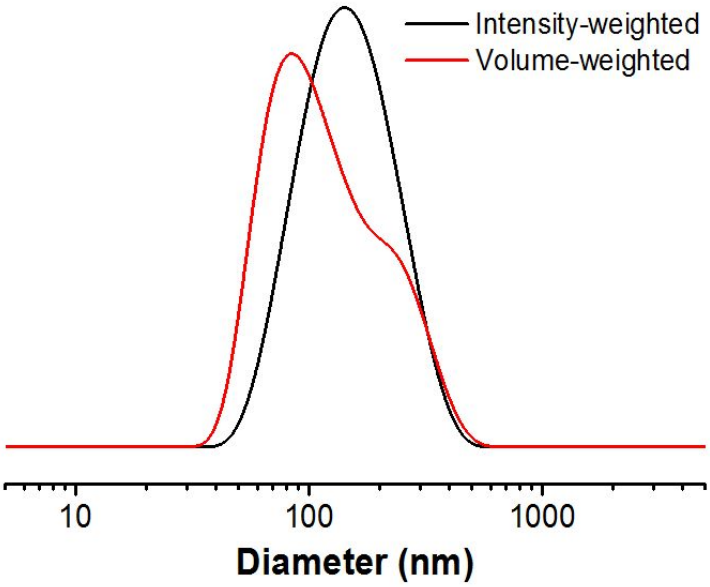

Figure S6. Hydrodynamic diameters of TR-cubes in saline solution by intensity (black curve) and by volume (red curve).

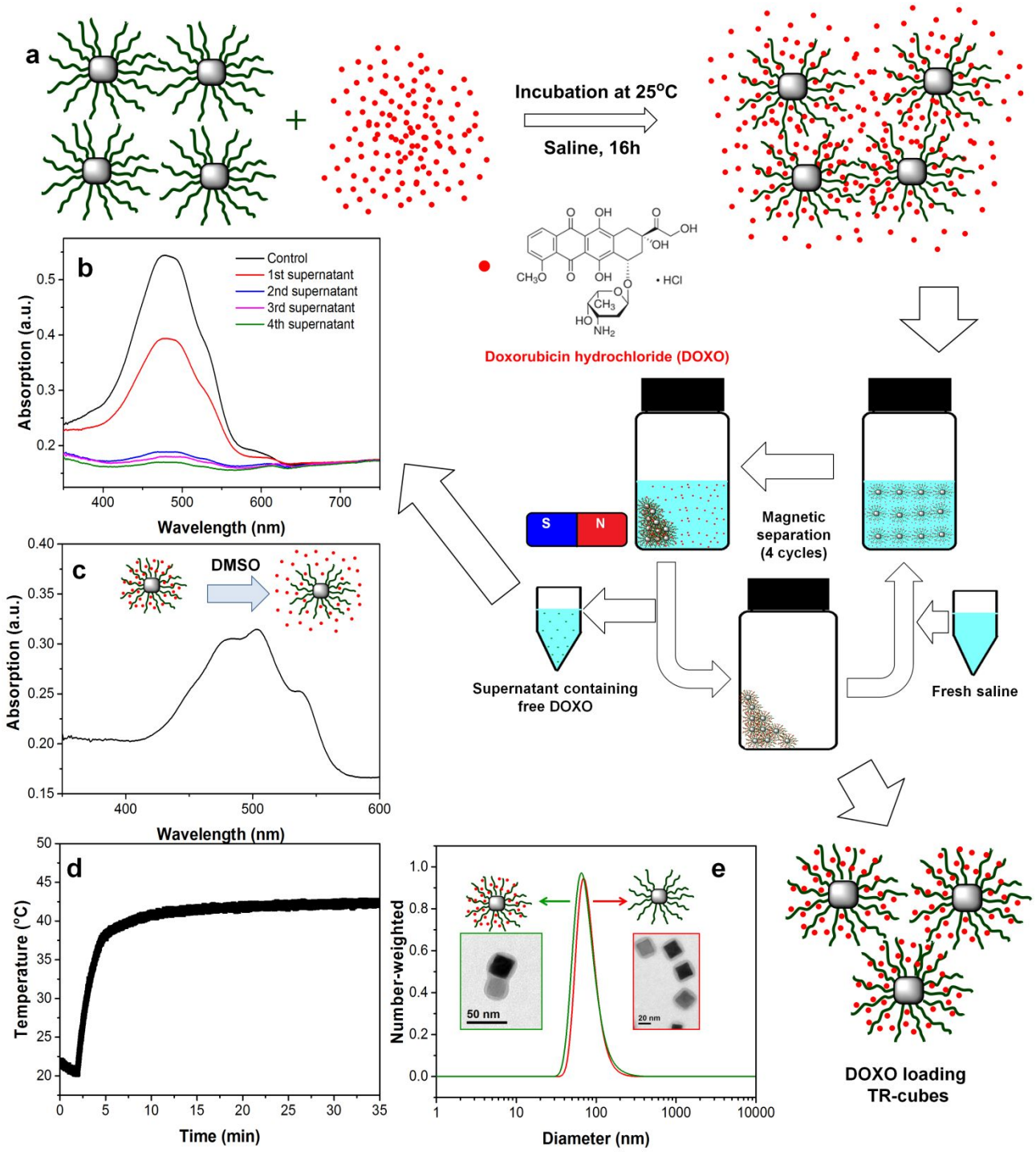

Figure S7. Characterization of DOXO-loaded TR-cubes. a. Schematic representation of DOXO loading on TR-cubes. **b.** The UV-vis absorption spectra of supernatants collected after different washing steps of magnetic cleaning. While the DOXO signal is clearly present in the first wash, it is completely eliminated by the fourth wash. The DOXO-loaded-TR-cubes that were collected by the magnet after the four washing steps were used for the experiments with cancer cells or in *in vivo* studies. **c.** The spectrum of the supernatant that was obtained after the DMSO release experiment. **d.** The heat profile of the solution of

DOXO-loaded-TR-cubes (edge 21.2 nm, Fe concentration 2.5 $g.L^{-1}$ / corresponding DOXO loaded amount was 47 µg per 1 mg of Fe) under MH at 11 $kA.m^{-1}$ and 105 kHz. **e.** The DLS size (number-weighted sprectra) of TR-cubes before (red) and after (green) the DOXO loading. (inset: the TEM micrographs of TR-cubes before (red frame) and after (green frame) the DOXO loading).

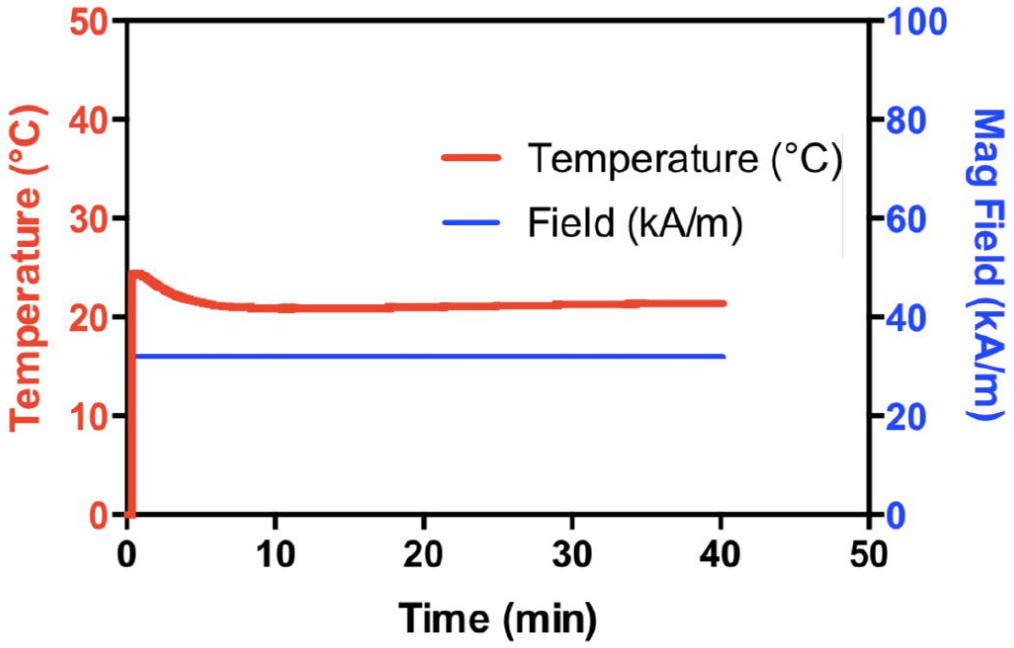

Figure S8. Temperature versus time profile measured on control A431 cells alone exposed to AMF (110 kHz) with no addition of nanoparticles. The temperature remained unchanged and stable around room temperature even when the maximum field amplitude was set at 32 kAm^{-1} a value that is higher than the one used in the *in vivo* MH study (11 kAm^{-1}).

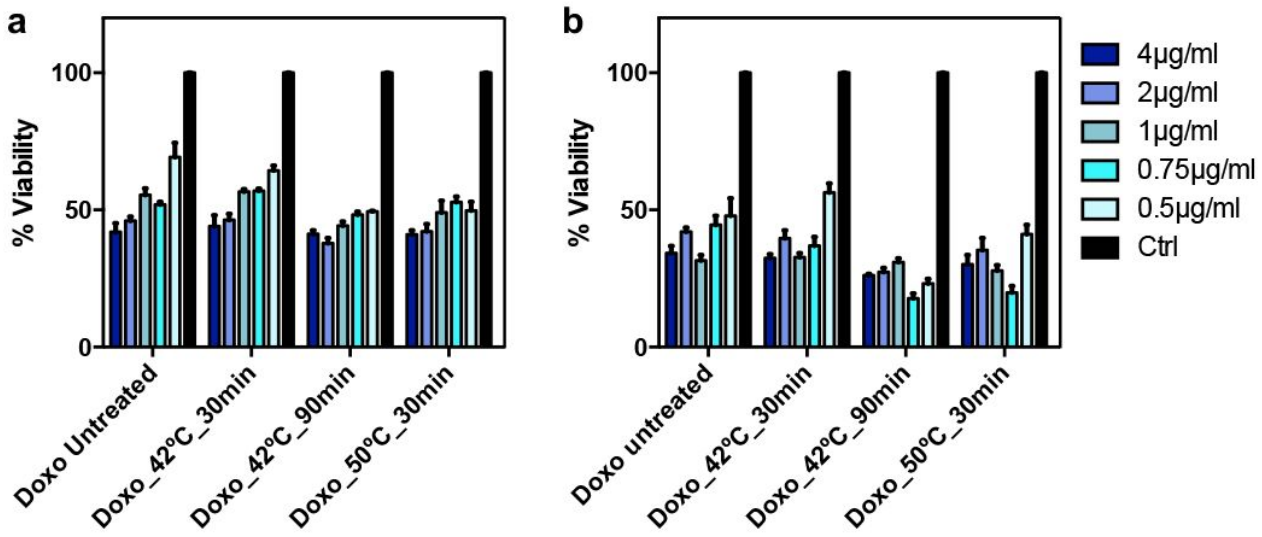

Figure S9. Effect of heat on chemotherapeutic efficiency of DOXO. Prestoblue® toxicity assay conducted on A431 epidermoid carcinoma cells exposed to untreated or pre-heat-treated DOXO at various temperatures. After additional incubation time of 24h (panel a) or 48 hours (panel b) viability was measured. **a.** At 24h, the viability of pre-heat treated Doxo groups at all temperature ranges studied, showed similar results to that of untreated Doxo group. **b.** Also at 48h, similar toxicity profiles to that of untreated DOXO were recorded for all the groups. These data provide evidence for the conservation of chemotherapeutic effect of our drug of interest even after exposure to higher temperature ranges, similar to the range experienced by Doxo in our MH treatment.

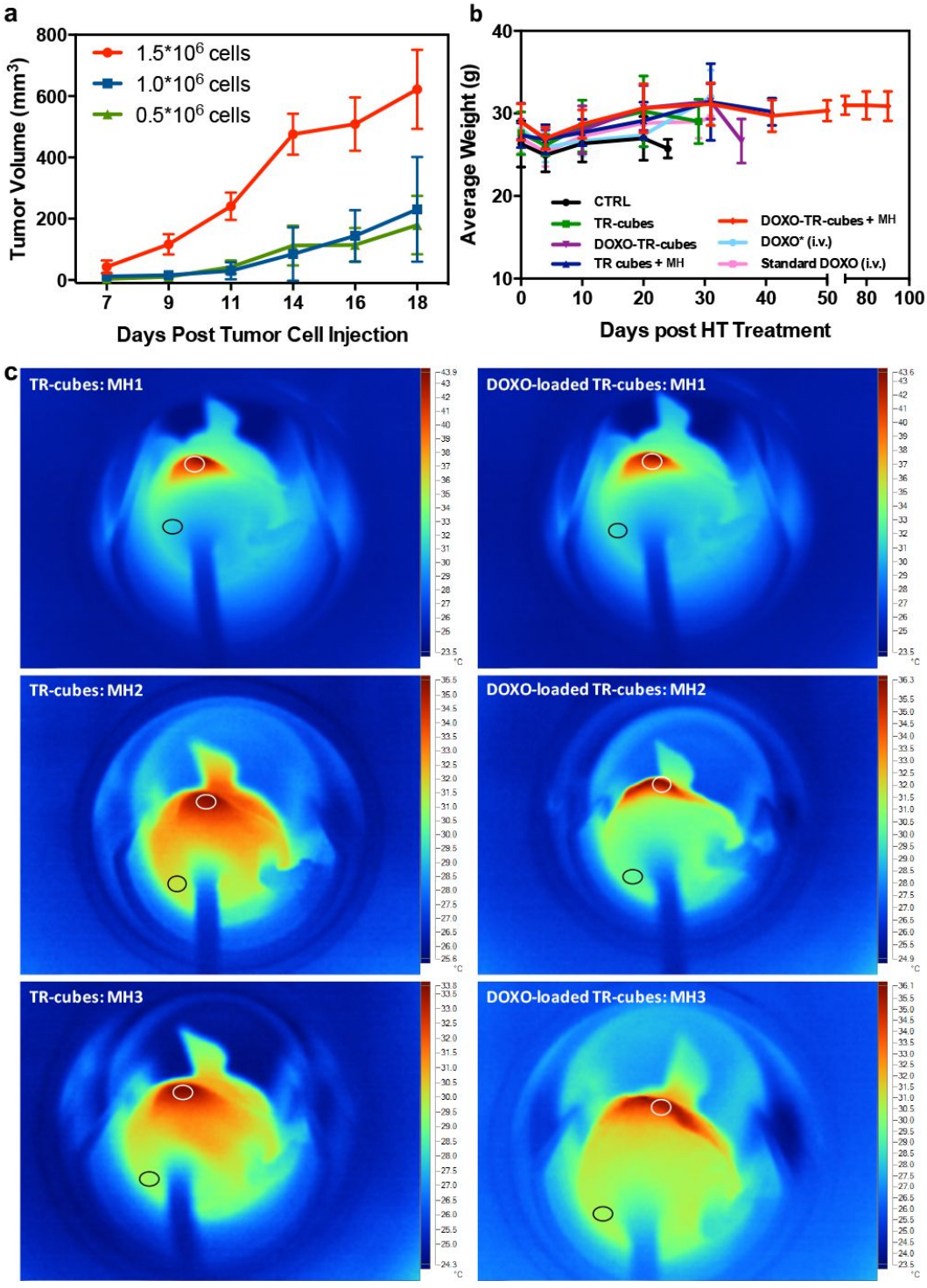

Figure S10. Cell injection, health status and heating profile of animals undergoing various treatments. a. Tumor growth curve analysis to fix the cell injection number per animal, showing that 1.5*10^6 cells in 100µL saline are optimum due to their consistent increase in tumor volume (n=6). **b.** Average weight graph indicating the health status of the animals in various group studies based on body weight (n=6). The TR-cube and DOXO-loaded TR-cube injections and MH did not affect the animals' weight, proving that

they were not under any distress during the course of treatment. **c.** Infrared images exhibiting the increase in the temperature of the tumor injected with TR-cubes (left panel) and DOXO-loaded-TR-cubes (right panel) under varying days of MH. The spreading of the heat profile from MH1 to MH3 shows the movement of the TR-cubes under AMF during MH treatment.

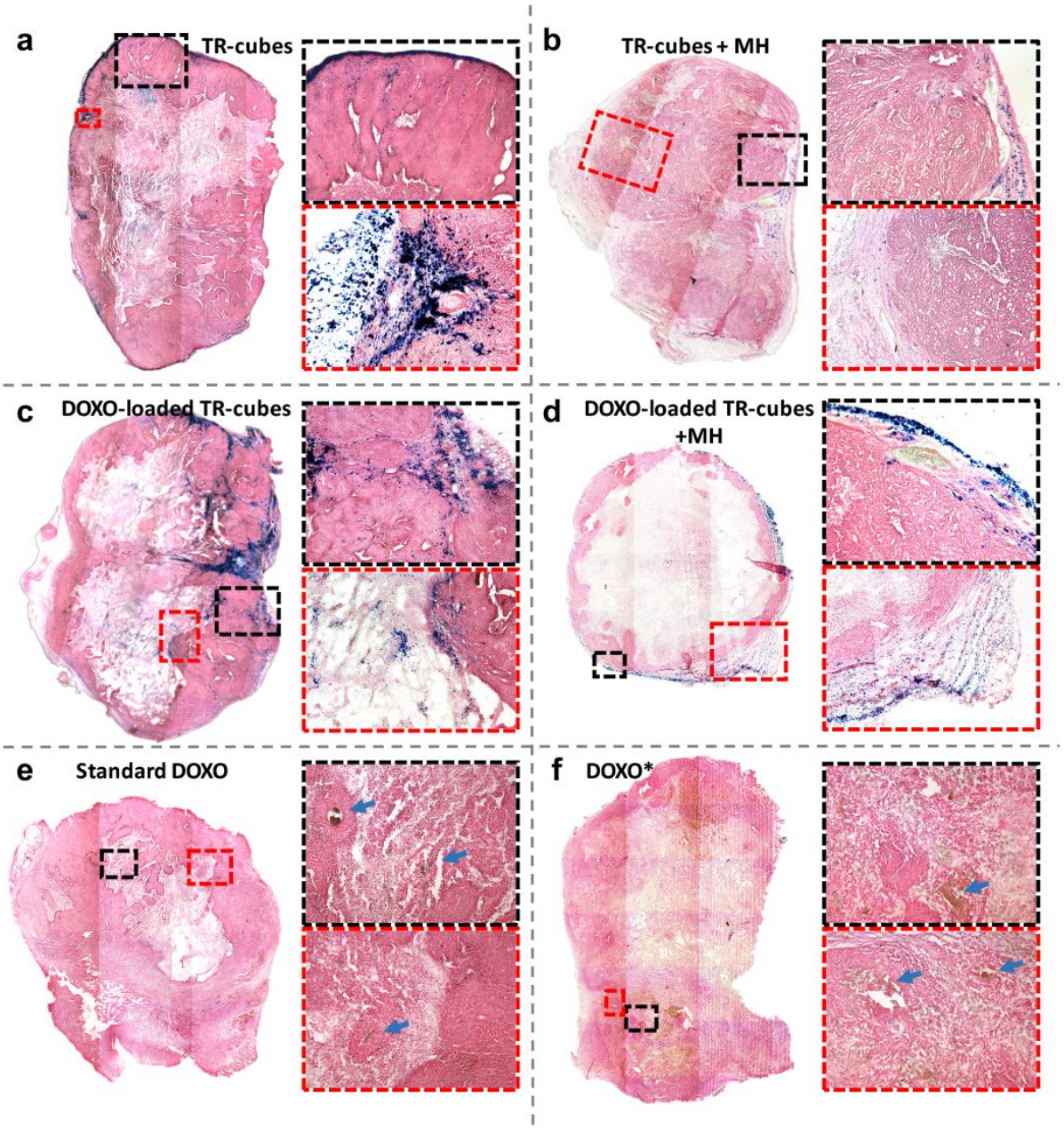

Figure S11. Histological analysis showing the difference in tumor morphology between non-treated and MH treated groups, and a comparison with standard chemotherapy. a-d. Virtually reconstructed tissues of tumor sections, stained with Prussian blue for iron and Fast Red for the cell nucleus and collagen, showing the presence of MNPs throughout the tumor and intact stroma in the case of the tissues treated with TR-cubes alone (**a**). TR-cubes + MH, showing signs of disruption in cellular integrity and loose collagen due to the MH treatment (**b**). An evident reduction in the stromal wall can be witnessed also in the case of the tumor treated with DOXO-loaded TR-cubes (**c**). This reduction is even more prominent and has comparatively less viable tumor mass for the DOXO-loaded TR-cubes + MH (**d**). **e-f.** Tumor sections of animals that

underwent standard chemotherapy by i.v. injection of 20mg/body weight DOXO (standard DOXO) **(e)** and an amount of DOXO that corresponded to the loaded amount in the TR cubes (DOXO*) **(f)**. The blue arrows indicate that blood vessels are stained darker due to the trapped Red Blood Cells that had been stained by Prussian Blue, showing a cellular scarcity and collagen destruction close to the blood vessels as a result of the DOXO accumulation, (i.v. injected) by Enhanced Permeation and Retention (EPR) effect. The DOXO-loaded-TR-cubes + MH treated groups showed more signs of cytotoxicity and destruction than the standard DOXO treated groups. The tissue slices were 10μm in thickness. All the data were collected from the tumor that had been resected from animals approximately 30days (28-32 days) post particle injection. Enlarged images are indicated with a black or red dashed box next to the fully reconstructed tissue image. The tumor slices were approximately 2cm in diameter except for (**d)** which was 0.6cm in diameter.

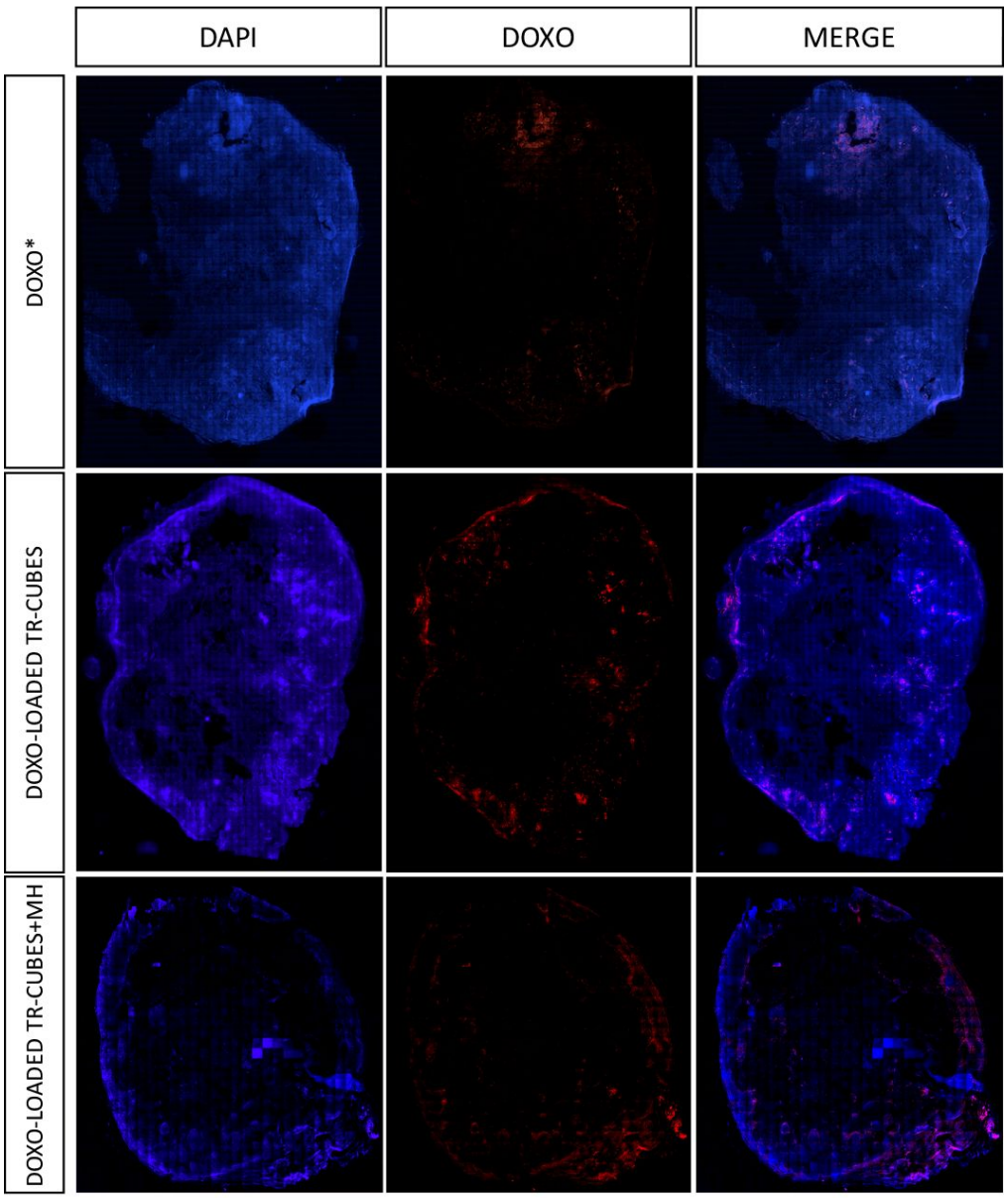

Figure S12. Confocal study to show the presence of DOXO in various groups under investigation. The slice of tissue retrieved from animals that had been treated with DOXO* showed that the DOXO signal was in close proximity to the blood vessels in the stroma of the tumor. The location of the blood vessels can be seen in Supplementary Fig. 6f. DOXO-loaded TR-cubes alone showed that the DOXO signal spread very close to the particles that were injected (compare to Supplementary Fig. 6), whereas the slice of animal treated with DOXO-loaded TR-cubes + MH showed that the DOXO spread well across the tumor. In this case, two thirds of the tumor section lacked cells, which was indicated by the poor DAPI signal, and the live cells at the periphery still contained DOXO. These findings explains and justifies the reason for complete tumor suppression in this group. Slices obtained were stained with ProLong™ Diamond antifade mountant with

DAPI, Ex:368nm Em:461nm; ii. DOXO representing the drug injected intravenously, Ex:480nm Em:580-590nm; iii. MERGE representing the combination of both DAPI and DOXO channel. The size of the tumor slices were approximately 2cm in diameter except for the DOXO-loaded TR-cubes + MH (which was 0.6cm), and they were studied from animals that were sacrificed approximately 30days post i.v. DOXO injection or particle injection.

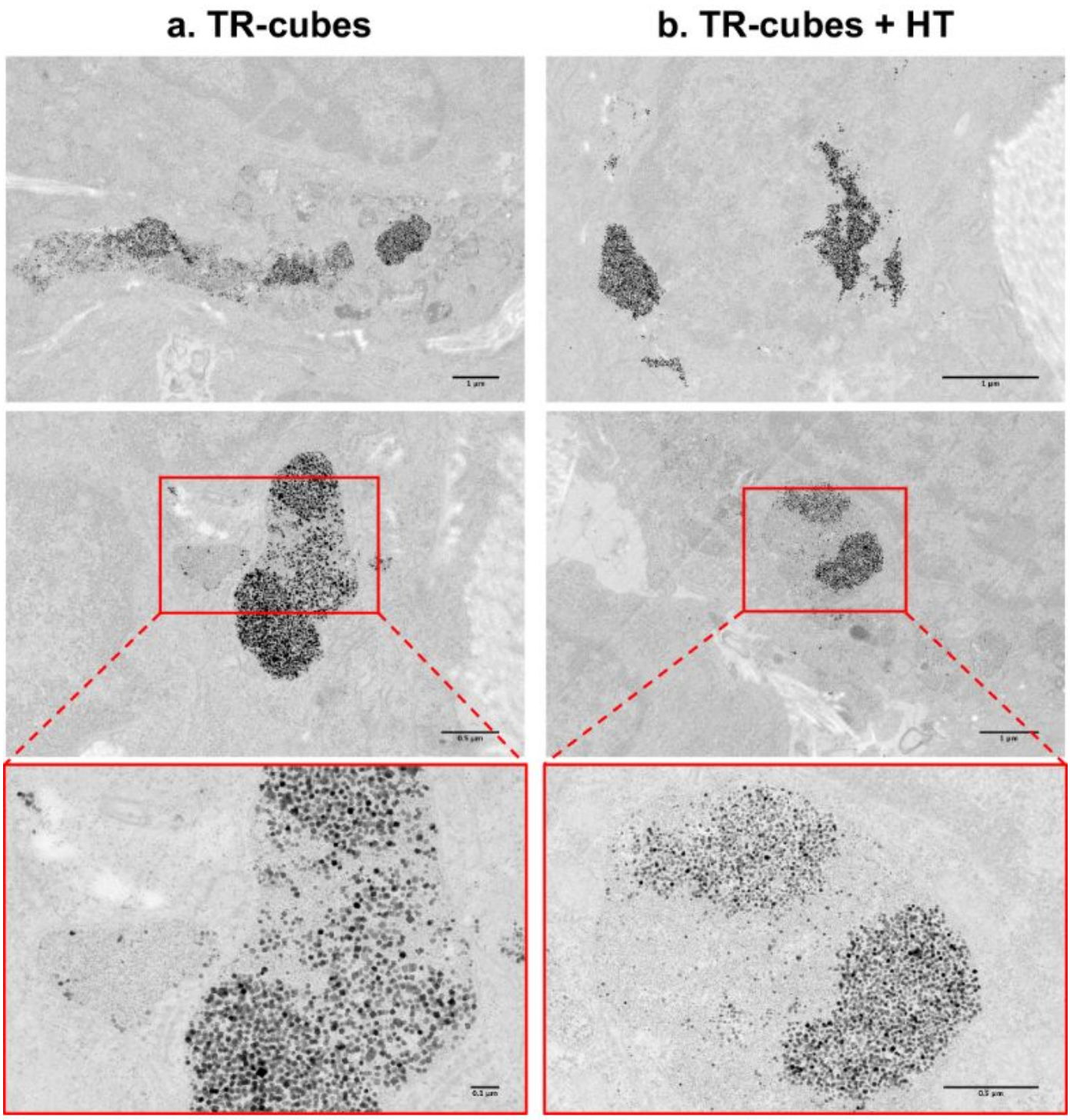

Figure S13 Transmission Electron Microscopy images showing TR-cubes (a) and TR-cubes + HT (b) treated tumor tissues at day 28, showing no aggregation or any special formation of the nanoparticles. However their original cubic shape seems modified, more round edges nanoparticles are seen in the magnified images.

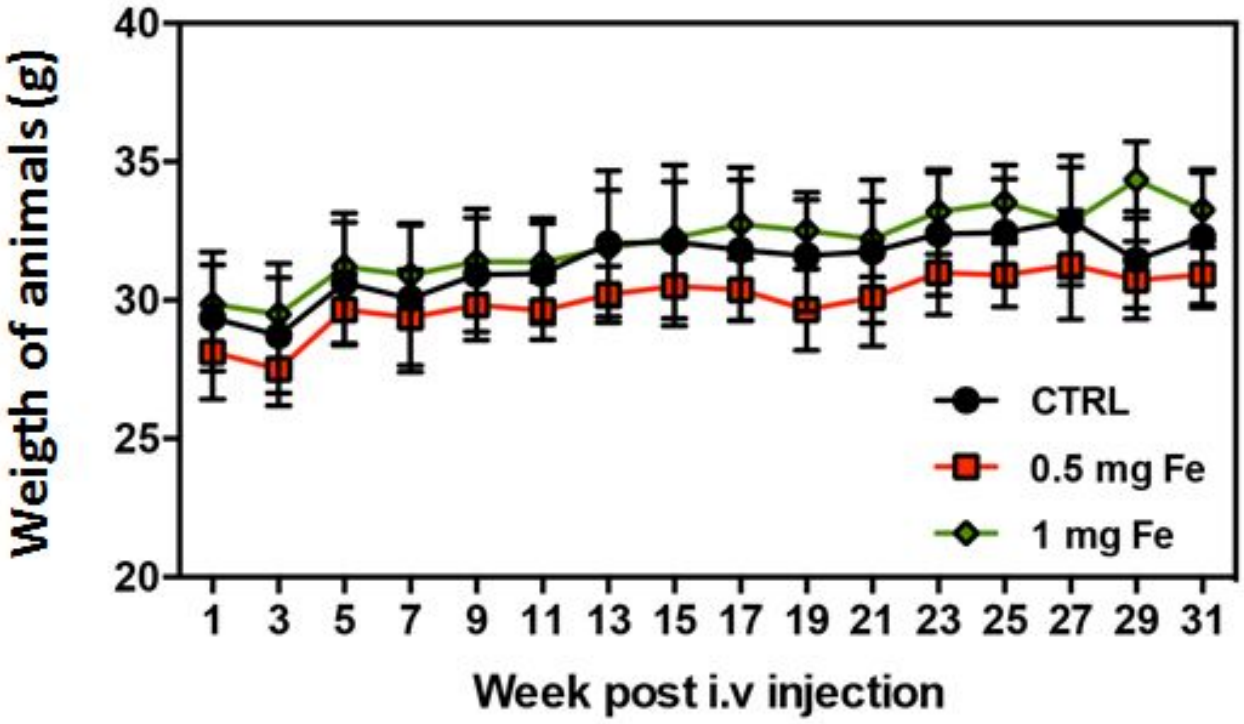

Figure S14. Weight graph showing the health status of animals injected intravenously with different concentration of TR-cubes (0.5 mg or 1mg Fe per animal). The graph shows clear indication that the animals injected with TR-cubes did not show any difference in weight from animals not injected with any nanoparticles (CTRL). Each data point represents the average weight of 6 animals with respective standard deviation (Mean ± SD). The plot represents animals observed for 31 weeks (8 months) which is the longest time point of our bio-distribution study"

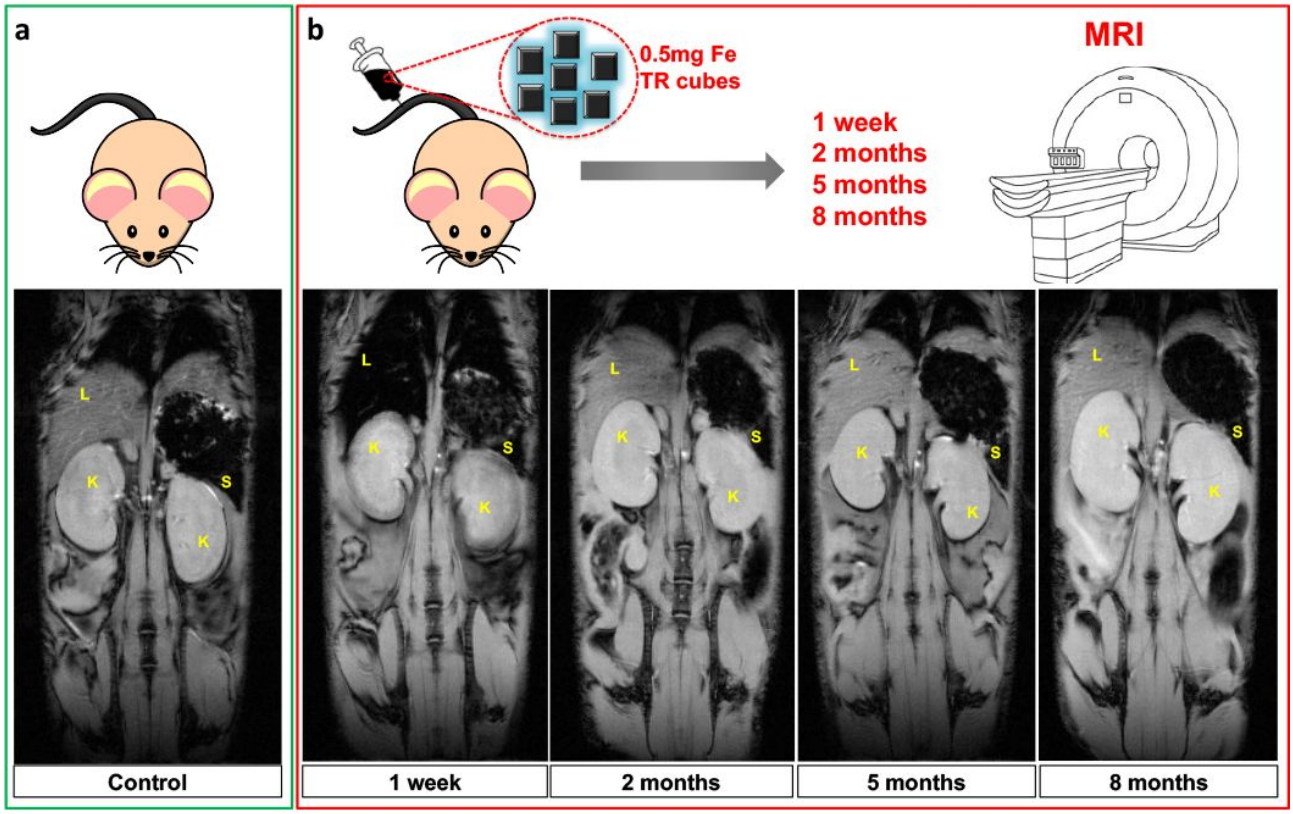

Figure S15 MRI: Follow-up of iron oxide nanocubes clearance over a period of 8 months from intravenous injection (0.5 mg iron) in healthy mice. A comparison of the gradient echo MRI scans (TE=5 ms) of a control mouse (a, green panel) and the mice injected with TR-cubes taken at 1 week, 2 months, 5 months and 8 months post-injection (b, red panel). These images show a pronounced hypo-intense signal in the liver (L), spleen (S) and kidney (K, note the dark kidney cortex representing initiation of clearance of the TR-cubes) at the 1 week time-point, that disappear at longer time-points, demonstrating the clearance of the magnetic nanoparticles.

Reference

(1) Fan, X.; Lin, L.; Dalsin, J. L.; Messersmith, P. B. Biomimetic anchor for surface-initiated polymerization from metal substrates. *J. Am. Chem. Soc* **2005**, *127*, 15843-15847.